1974

Heat transfer characteristics of a rotating two-phase thermosyphon.

Tucker, Richard Steven.

Monterey, California. Naval Postgraduate School

HEAT TRANSFER CHARACTERISTICS OF A ROTATING TWO-PHASE THERMOSYPHON

Richard Steven Tucker

NAVAL POSTGRADUATE SCHOOL
Monterey, California

THESIS

HEAT TRANSFER CHARACTERISTICS
OF A
ROTATING TWO-PHASE THERMOSYPHON

by

Richard Steven Tucker

September 1974

Thesis Advisor: P.J. Marto

Approved for public release; distribution unlimited.

UNCLASSIFIED
SECURITY CLASSIFICATION OF THIS PAGE (When Data Entered)

REPORT DOCUMENTATION PAGE		READ INSTRUCTIONS BEFORE COMPLETING FORM
1. REPORT NUMBER	2. GOVT ACCESSION NO.	3. RECIPIENT'S CATALOG NUMBER
4. TITLE (and Subtitle) Heat Transfer Characteristics of a Rotating Two-Phase Thermosyphon		5. TYPE OF REPORT & PERIOD COVERED Master's Thesis; September 1974 6. PERFORMING ORG. REPORT NUMBER
7. AUTHOR(s) Richard Steven Tucker		8. CONTRACT OR GRANT NUMBER(s)
9. PERFORMING ORGANIZATION NAME AND ADDRESS Naval Postgraduate School Monterey, California 93940		10. PROGRAM ELEMENT, PROJECT, TASK AREA & WORK UNIT NUMBERS
11. CONTROLLING OFFICE NAME AND ADDRESS Naval Postgraduate School Monterey, California 93940		12. REPORT DATE September 1974 13. NUMBER OF PAGES 57
14. MONITORING AGENCY NAME & ADDRESS (if different from Controlling Office) Naval Postgraduate School Monterey, California 93940		15. SECURITY CLASS. (of this report) Unclassified 15a. DECLASSIFICATION/DOWNGRADING SCHEDULE

16. DISTRIBUTION STATEMENT (of this Report)

Approved for public release; distribution unlimited.

17. DISTRIBUTION STATEMENT (of the abstract entered in Block 20, if different from Report)

18. SUPPLEMENTARY NOTES

19. KEY WORDS (Continue on reverse side if necessary and identify by block number)

Heat Transfer Characteristics
Thermosyphon
Condensation
Heat Pipe

20. ABSTRACT (Continue on reverse side if necessary and identify by block number)

A rotating two-phase thermosyphon fitted with a copper condenser section was tested at 700, 1400 and 2800 RPM using water, ethanol and freon 113 as working fluids. Both experimental and theoretical heat transfer rates were determined. Agreement between theory and experiment was good at low rotational speeds and improved as the rotational speed increased.

DD FORM 1 JAN 73 1473 EDITION OF 1 NOV 65 IS OBSOLETE
S/N 0102-014-6601 |
(Page 1)

UNCLASSIFIED
SECURITY CLASSIFICATION OF THIS PAGE (When Data Entered)

(20. ABSTRACT continued)

The effects of having noncondensable gases present in the condenser were evaluated experimentally using water as a working fluid. It was found that a small amount of non-condensable gas slightly degraded performance at low rotational speeds but significantly lowered the heat transfer rates at high rotational speeds.

Heat transfer rates with water were increased by promoting dropwise condensation, using a thin coating of silicone grease. These results, though consistently higher than results for filmwise condensation, showed poor repeatability.

Heat Transfer Characteristics of a Rotating Two-Phase Thermosyphon

by

Richard Steven Tucker
Lieutenant, United States Navy
B.S.M.E., University of Nevada, 1968

Submitted in partial fulfillment of the requirements for the degree of

MASTER OF SCIENCE IN MECHANICAL ENGINEERING

from the

NAVAL POSTGRADUATE SCHOOL

September 1974

ABSTRACT

A rotating two-phase termosyphon fitted with a copper condenser section was tested at 700, 1400, and 2800 RPM using water, ethanol and freon 113 as working fluids. Both experimental and theoretical heat transfer rates were determined. Agreement between theory and experiment was good at low rotational speeds and improved as the rotational speed increased.

The effects of having noncondensable gases present in the condenser were evaluated experimentally using water as a working fluid. It was found that a small amount of non-condensable gas slightly degraded performance at low rotational speeds but significantly lowered the heat transfer rates at high rotational speeds.

Heat transfer rates with water were increased by promoting dropwise condensation, using a thin coating of silicone grease. These results, though consistently higher than results for filmwise condensation, showed poor repeatability.

TABLE OF CONTENTS

I. INTRODUCTION

A. THE ROTATING TWO-PHASE THERMOSYPHON

The rotating two-phase thermosyphon also called a rotating noncapillary heat pipe, is a heat transfer device that can be used to cool a rotating component such as a turbine shaft or a high speed bearing. This device, as illustrated in Figure 1, consists of a truncated cone-shaped condenser, the large end of which opens into a cylindrical-shaped evaporator. This closed system contains a volume of working fluid sufficient to prevent burnout of the evaporator.

When the thermosyphon is rotated above a critical speed, the working fluid forms an annulus in the evaporator. Heat input to the evaporator causes some of the working fluid to vaporize and this vapor is drawn into the condenser. External cooling of the condenser allows the vapor to condense on the inner condenser wall. The centrifugal force due to the rotation has a component acting along the condenser wall which accelerates the condensate back into the evaporator.

B. BACKGROUND

A theoretical model of the thermosyphon operation, using film condensation theory was developed by Ballback [1], and was subsequently modified by Daley, Newton, and Schafer [2,3,4]. The approximate solution of the model consists of

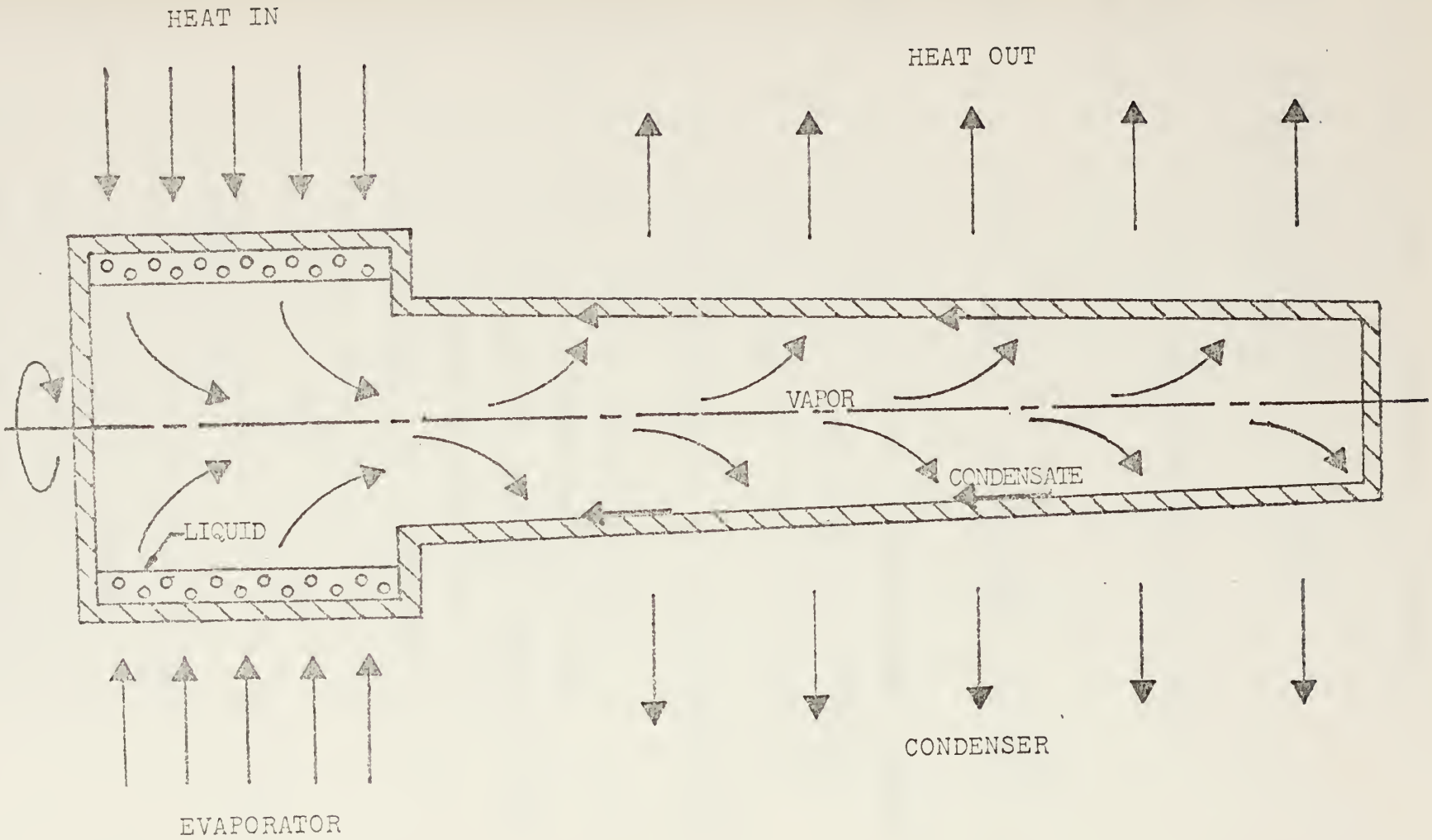

Figure 1. Schematic Drawing of a Rotating Two-Phase Thermosyphon

a first order ordinary differential equation:

$$\frac{dv}{dx} = \frac{2(R_o + x \sin \phi)(T_s - T_w(x))}{\rho_v \left[\frac{\delta(x)}{k_f} + \frac{t}{k_w} \right] R^2 h_{fg}} - \frac{2v \sin \phi}{R}$$

which must be solved simultaneously with a cubic equation:

$$\frac{\delta^3}{3} R \sin \phi \left[\rho_f \omega^2 R + \frac{2\rho_v v^2}{R} \right] - \rho_v v^2 f\left(R \frac{\delta^2}{4}\right) - \rho_v v \frac{\mu_f R^2}{2\rho_f} = 0$$

where f = friction factor in the vapor space, dimensionless

h_{fg} = latent heat of vaporization in Btu/lbm.

k_f = thermal conductivity of the liquid in Btu/hr.ft.°F

k_w = thermal conductivity of the condenser wall in Btu/hr.ft.°F

q = heat transfer rate in Btu/hr.

$R(x)$ = internal condenser radius in feet

R_o = minimum internal condenser radius in feet

T_s = vapor saturation temperature in °F

$T_w(x)$ = outer condenser wall temperature in °F

t = condenser wall thickness in feet

$v(x)$ = velocity of vapor in ft./sec.

x = coordinate measuring distance along condenser length in feet

$\delta(x)$ = coordinate film thickness in feet

ϕ = half cone angle in radians

ρ_f = density of the liquid in lbm/ft.^{3}

ρ_v = density of the vapor in lbm/ft.^{3}

μ_f = viscosity of the liquid in lbm/ft.sec.

ω = angular velocity in radians/sec.

Once $\delta(x)$ is known, the heat transfer rate can be calculated from the energy equation:

$$dq = \frac{2\pi(R_o + x \sin \phi)(T_s - T_w(x))\, dx}{\frac{\delta(x)}{k_f} + \frac{t}{k_w}}$$

A computer program which solves these equations was developed by Schafer [4] to determine the predicted values of the heat transfer rate. This program was used to establish the theoretical values of heat transfer in this work.

Experiments using the thermosyphon have been performed by Newton [3], Woodard [5], and more recently by Schafer [4]. Three major problems with the previous experiments were (a) insufficient instrumentation of the outer condenser wall, (b) excessive electronic noise levels on the condenser wall thermocouples, and (c) vacuum leaks in the sealed thermosyphon which allowed noncondensable gases to enter the system.

C. THESIS OBJECTIVES

The principal objectives of this thesis were to (a) instrument a copper condenser and measure the outer wall temperature profile, (b) eliminate the noise level present on the condenser allowing accurate temperature measurements, (c) establish a leak free system to allow

evaluation of the effects of noncondensable gases on system performance, (d) compare the performance predicted by the theoretical analysis to the experimental performance using a copper condenser section and using water, ethanol and freon 113 as working fluids, (e) compare the performance of the copper condenser to the performance of both the copper and stainless steel condenser performance obtained by Schafer [4], and (f) compare thermosyphon performance for filmwise condensation to the performance for dropwise condensation.

II. EXPERIMENTAL EQUIPMENT

A. DESCRIPTION OF EQUIPMENT

Heat input to the evaporator was provided by a resistance heating element wrapped around the evaporator as shown in Figure 2. Power was supplied to this heater from a 220 volt A.C. 200 ampere source through a 100 ampere breaker to eight graphite brushes riding on two brass collector rings which were wired directly to the heater element. Resistance load banks in series with the heater element were used to control the power to the heater. A series-parallel arrangement of six load bank units allowed the power to be varied from 0.20 kilowatts to 8.33 kilowatts. Higher power could have been achieved by using additional load banks.

The condenser was surrounded by a sealed insulated box. Garlock seals at each end of the condenser kept the cooling water from leaking out. Nozzles placed around the inside of the box sprayed filtered tap water on the outer condenser surface and drains in the bottom of the box collected the cooling water. The inlet and outlet cooling water temperatures were measured along with the cooling water flow rate.

The thermosyphon was rotated in two bearings by a three phase variable speed motor with a v-belt drive. A sixty tooth gear mounted on the thermosyphon drive shaft near a

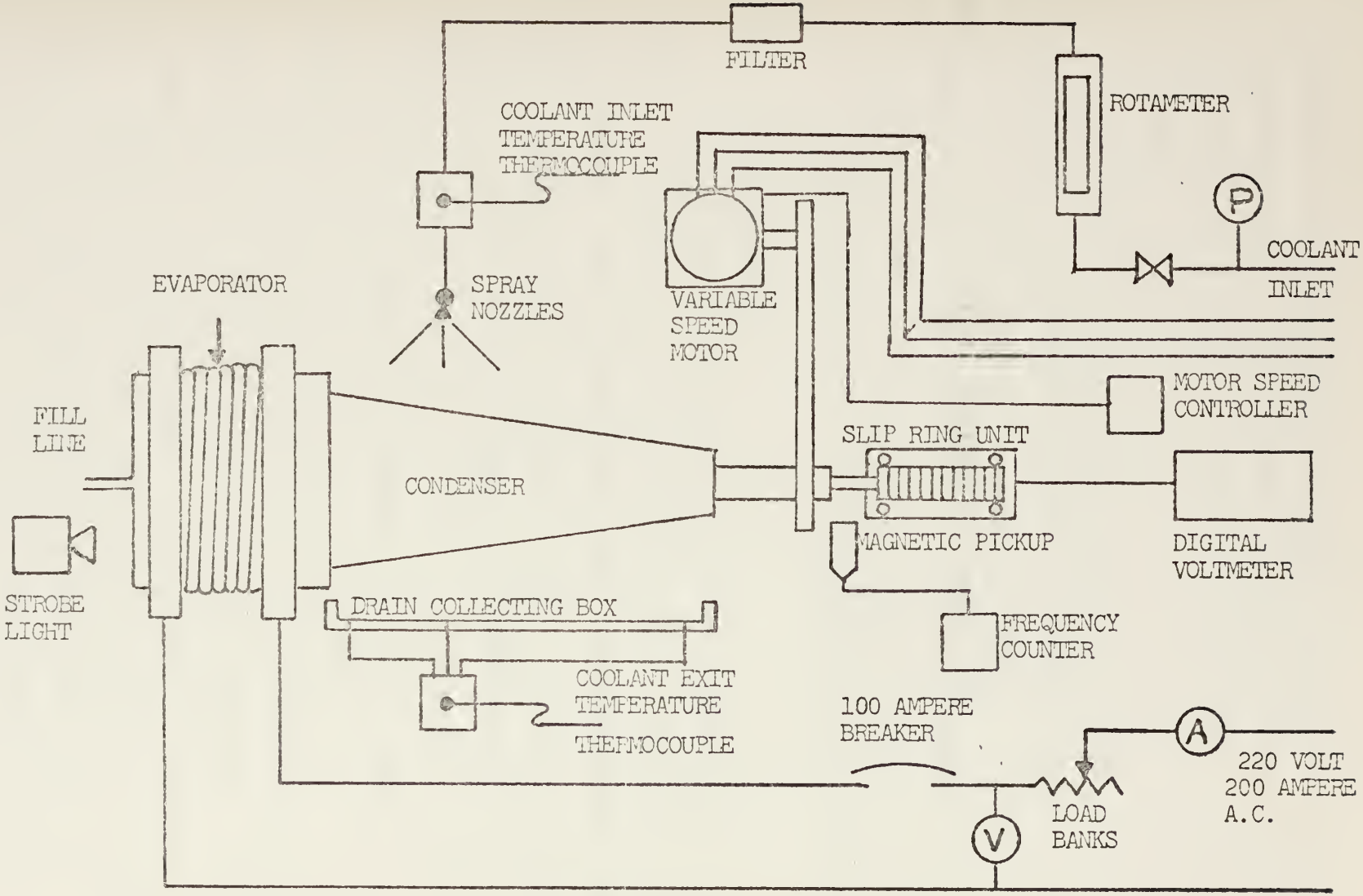

Figure 2. Schematic Drawing of Experimental Equipment

variable reluctance pickup provided a means of measuring rotational speed. The number of teeth per second counted was numerically equal to the rotational speed in revolutions per minute.

The end of the evaporator opposite the condenser contained a viewport consisting of two glass disks with an air space between them to prevent fogging. A strobe light shined through this viewport and when synchronized to the rotational speed, allowed observation of the boiling action in the fluid annulus and the condensate in the condenser.

B. INSTRUMENTATION

All thirteen thermocouples used were made from 30 gage Kapton insulated, copper-constantan wire. They were made by fusing a bead between the copper and constantan leads with an argon arc thermocouple welder. The two thermocouples used to measure saturation temperature in the evaporator were sheathed in four inch lengths of .0625 inch diameter stainless steel tubing. The end of the tube containing the bead was sealed with solder.

The thermocouple leads were cut to length and soldered into the male end of one of three pin connectors. Teflon coated copper and constantan leads from the rotating disks of the mercury slip ring unit were run down the length of the hollow drive shaft and out of the shaft near the condenser end piece. Here they were soldered into the female end of one of the three pin connectors which were

then mounted to the condenser end piece. The stationary portion of the slip ring unit was connected via copper constantan wiring, to a Hewlett Packard data acquisition system which consisted of an integrating digital volt meter, a guarded data amplifier, a crossbar scanner, and a digital recorder. In addition, an oscilloscope was used to observe the electronic noise level of the thermocouple voltage signals. This completed the assembly of this portion of the system.

The condenser wall and vapor space thermocouples were then calibrated through the system described above. This meant that the entire system, rather than just the thermocouples, was being calibrated. Calibration was performed in a Rosemont constant temperature bath using a platinum resistance thermometer as a standard. A graph of thermocouple error as a function of thermocouple reading was plotted for each thermocouple channel to be used to correct experimental readings.

The inlet cooling water thermocouple was sheathed in a four inch length of .0625 inch diameter stainless stell tubing and the bead end was sealed with low temperature silicone rubber. The outlet cooling water thermocouple was actually five thermocouples, each sheathed in a short length of .0625 inch diameter stainless steel tubing. All five leads were then passed through a four inch length of .125 inch diameter stainless steel tubing and then connected in parallel to provide an average reading. The leads from

these thermocouples led to a thermally insulated junction board. Copper-constantan wire connected this junction board to the data acquisition system.

These cooling water thermocouples were calibrated in an insulated container filled with distilled water using a set of gas filled mercury thermometers accurate to ±.1° Fahrenheit as a standard. Again a plot of thermocouple error versus thermocouple reading was made.

The rotameter used to measure the flow rate of the cooling water was calibrated by pumping water through the cooling water system and noting the rotameter reading. The flow was directed into a container for a measured amount of time and the water in the container was weighed. A plot of rotameter reading versus mass flow rate completed the calibration.

The thermocouples were now installed on the equipment. Condenser wall thermocouples were soldered into slots cut into the copper condenser at nine longitudinal positions, 0.03, 2.08, 4.05, 5.61, 6.98, 7.44, 7.84, 8.31, and 8.69 inches from the closed end of the condenser. The vapor space thermocouple sheaths were soldered into holes going from the cooling water space through the evaporator wall into the evaporator vapor space. Cooling water thermocouples were installed in their respective mixing boxes using fittings which sealed around the stainless steel tubes.

C. THERMOCOUPLE NOISE REDUCTION

A systematic noise search indicated that significant noise levels on the condenser wall thermocouple signals appeared only when the thermosyphon was rotating and power was applied to the heater element. Noise increased with both increased rotational speed and increased heater power. Inspection of the collector rings and graphite brushes revealed a significant amount of runout in the collector rings; the brushes were making contact only over a fraction of their total surface area.

The brushes were removed and the collector rings were machined to reduce the runout to about one thousandth of an inch. The brushes were sanded to the exact contour of the collector rings and both rings and brushes were polished. The brush assembly was reinstalled and the equipment was run while a polishing compound was applied to the collector rings to facilitate the wearing in of the brushes to the rings.

Every brush was now making contact over nearly all of its available area and while the noise level was significantly reduced, it was still unacceptably high. Increased rotational speed was still accompanied by increased noise but increasing power no longer seemed to change the noise level.

Next, the condenser was electrically grounded by grounding the copper lead of one of the thermocouples soldered to its surface. This significantly reduced the

noise on all thermocouples except the one providing a ground. To avoid this problem, the copper leads of two condenser wall thermocouples were wired through a three way switch to ground in such a way that either one or the other or neither thermocouple could be used to supply the ground.

It was further discovered that by installing a twenty microfarad precision capacitor across the digital voltmeter input, the remaining noise could be reduced to less than twenty microvolts which was considered an acceptable level. The digital voltmeter integrated out the remaining noise and presented steady, accurate thermocouple readings.

D. SYSTEM LEAK ELIMINATION

The system was sealed and pressure tested using nitrogen gas at 30 pounds per square inch, gage pressure. A rapid loss of pressure revealed the presence of leaks. Reseating "O" ring seals and applying soap to joints failed to pinpoint the leaks. Pressure testing was abandoned in favor of a vacuum leak detector.

This vacuum leak detector operated by pumping gases from the system through an electronic tube with a helium sensitive grid. Leaks could then be pinpointed by blowing helium in the immediate vicinity of a suspected leak and observing the reaction of the helium detector tube. Leaks in the evaporator solder joints and in one evaporator instrumentation hole were found and repaired. The heat pipe was then pumped down to the maximum vacuum the test

equipment could reach and the area surrounding the heat pipe was saturated with helium. No helium was detected by the helium detector so the system was determined to be leak free.

E. INSTALLATION OF THE VENT

The final modification was the installation of the vent, as shown in Figure 3. The vent was a one eighth inch hole drilled through the condenser endpiece which allowed the condenser to be vented to the atmosphere. This hole was internally threaded the first part of its length, then its diameter was reduced leaving a shoulder to act as an "O" ring seat. The smaller hole then continued into the condenser. A set screw with an "O" ring mounted on its end was screwed into the threaded portion of the hole until the "O" ring seated on the shoulder, closing the vent. The vent could then be opened by simply backing out the set screw while the thermosyphon was stationary.

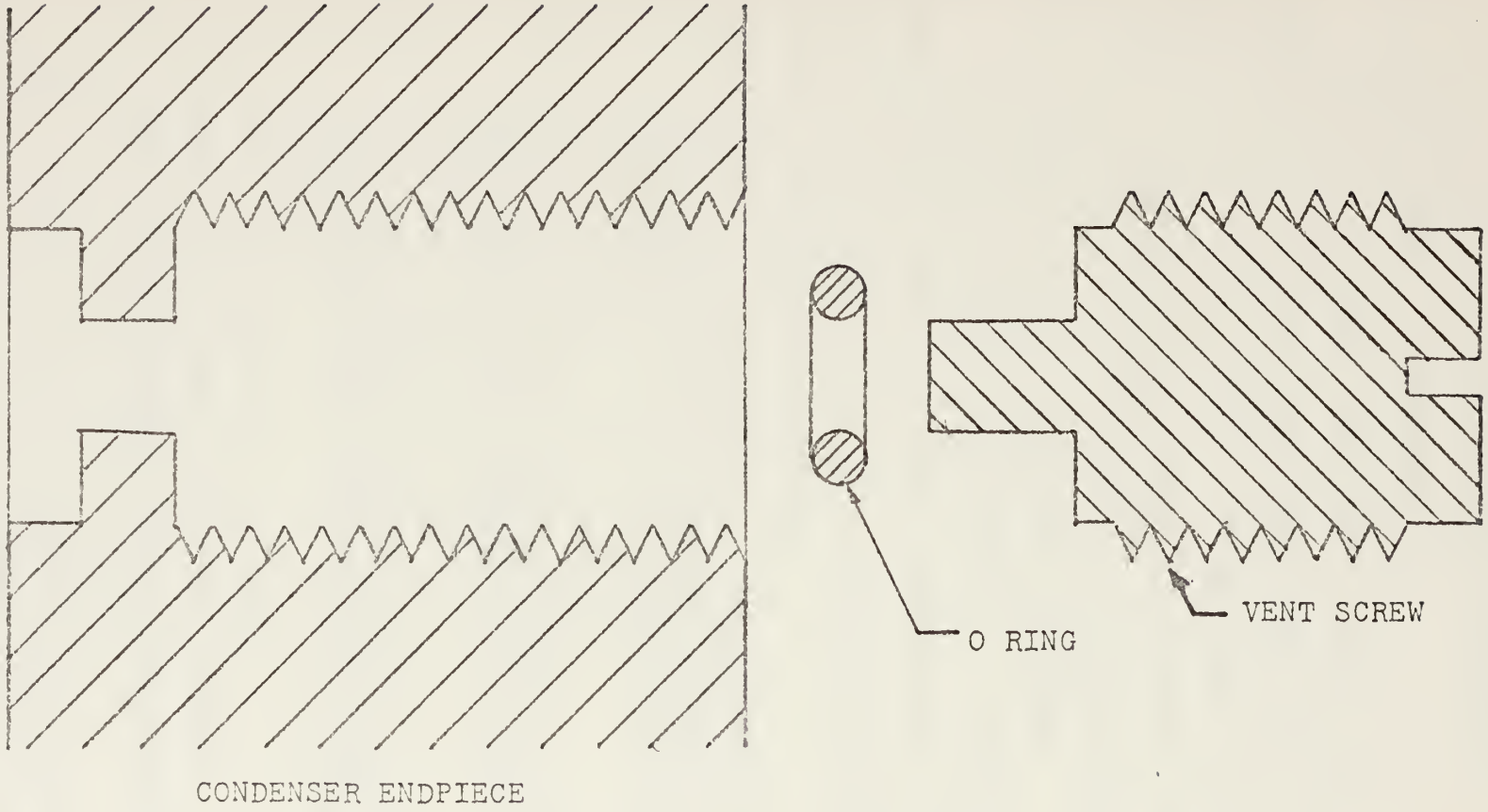

Figure 3. Schematic Drawing of the Venting System

III. EXPERIMENTAL PROCEDURE

A. PREPARATION OF CONDENSER WALL

Prior to running, the inner condenser wall was mechanically cleaned with emery paper then polished with successively finer grades of emery paper, alumina polishing compound, and finally a slurry of jeweler's rouge. It was not necessary to do this prior to every run but only when the condenser became excessively oxidized.

To obtain filmwise condensation, a chemical cleaning procedure was used which was a modification of a procedure used in preparing copper for electroplating [6]. The steps in the cleaning are as follows:

a. Tilt the thermosyphon to a nearly vertical position.
b. With the evaporator viewports removed, fill the condenser with trichloroethylene and scrub with a bottle brush.
c. Drain and rinse with tap water.
d. Fill the condenser with a mixture of equal parts of ethyl alcohol and fifty percent solution of sodium hydroxide warmed to 180°F.
e. Drain and rinse with tap water.
f. Fill the condenser with ten percent sulfuric acid solution and scrub with a bottle brush. Do not leave the sulfuric acid in the condenser longer than five minutes.
g. Drain and rinse with tap water.
h. Rinse three times with distilled water.
i. Tilt the thermosyphon back to the horizontal position and allow the interior to dry.

The condenser could be prepared for dropwise condensation by applying a thin coat of silicone vacuum grease evenly over the inner condenser surface.

B. FILL PROCEDURES

Before filling, the thermosyphon was sealed. The glass end windows were cleaned with an antifogging glass cleaner and installed with the appropriate "O" ring, gaskets and retainer ring. The bolts of the retainer ring were torqued to thirty inch-pounds in ten inch-pound steps to avoid cracking the glass windows.

The standard filling procedure utilized the fill apparatus illustrated in Figure 4, connected to the vacuum system and to the thermosyphon as shown. With the apparatus in position one, the vacuum and thermosyphon valves were opened allowing the thermosyphon to be evacuated, usually down to a pressure of 5×10^{-6} millimeters of mercury. The thermosyphon valve was then closed and the fill apparatus was rotated to position 2. The reservoir valve was then opened, allowing the vacuum to degas the working fluid for three to five minutes. Once the working fluid was completely degassed, the vacuum valve was closed and the fill system was returned to position one. The fill system was then raised above the thermosyphon and the thermosyphon valve was opened allowing the working fluid to flow into the thermosyphon. All valves on the filling system were closed as soon as all the working fluid was in the thermosyphon. The glass tube through the glass end windows was sealed off by heating a small section of the tube with an oxyacetylene torch until the glass melted. The vacuum within the glass tube caused the molten glass to collapse inward, sealing the tube.

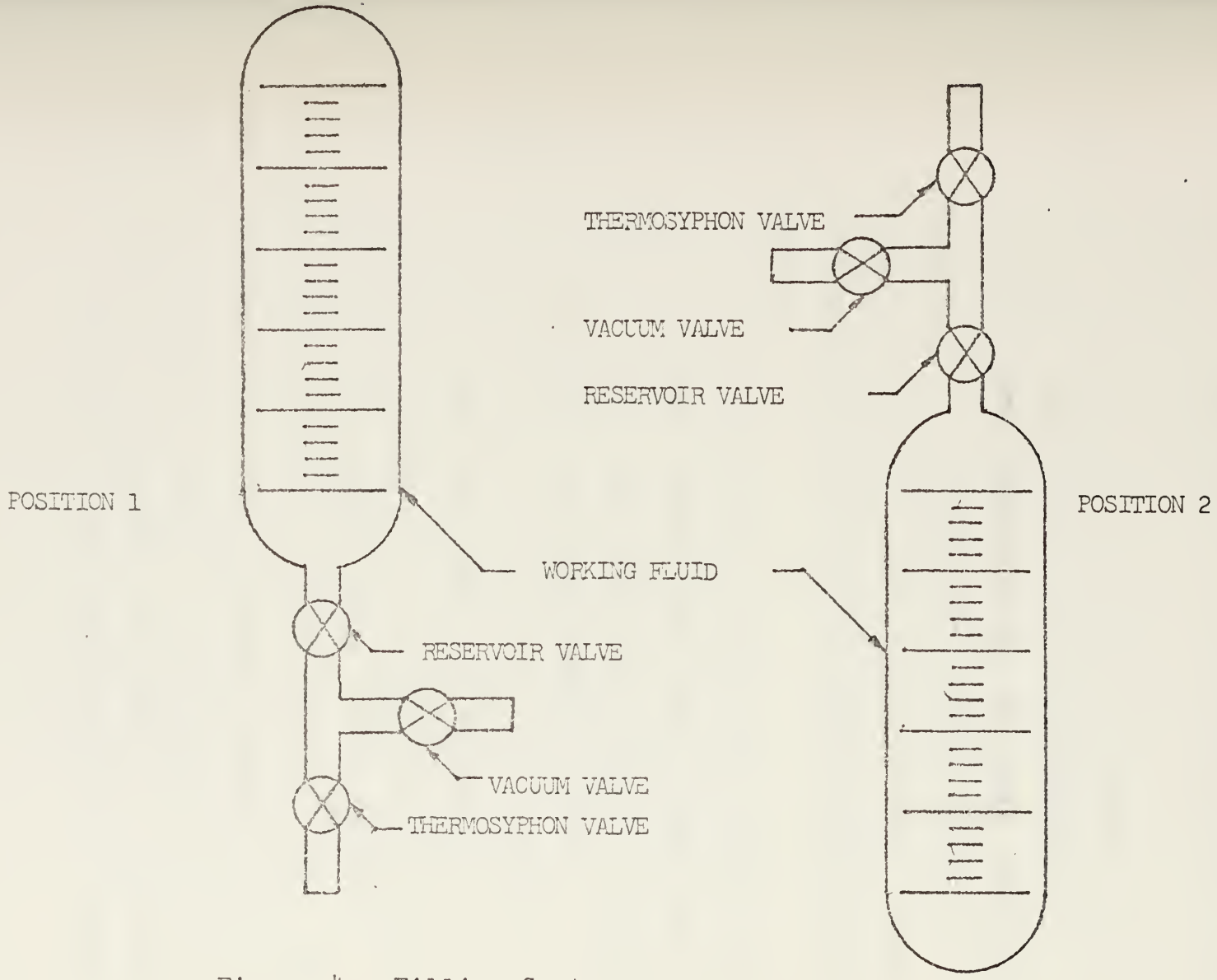

Figure 4. Filling System

In most of the runs, this standard fill procedure was followed by a venting procedure. Venting was accomplished in the following manner:

a. Tilt the thermosyphon to a 45° angle with the evaporator end down.

b. Apply .25 kilowatts of power to the heater until the saturation temperature in the thermosyphon is approximately 10 degrees above the known saturation temperature of the particular working fluid at atmospheric pressure. This means that the internal thermosyphon pressure is now slightly above atmospheric pressure.

c. Back out the vent screw allowing some working fluid vapor to escape. Control the flow of the vapor with the vent screw, being careful to keep the pressure in the thermosyphon above atmospheric pressure.

d. Vent for three to five minutes. Turn off the electrical power and reseat the vent screw.

e. Return the thermosyphon to the horizontal position and turn on the cooling water to the condenser.

Another fill procedure used was the fill, pump, and seal procedure. The working fluid was placed in the thermosyphon at atmospheric pressure. The vacuum system was then connected and the thermosyphon was pumped for approximately one hour. The system was then sealed as in the standard run.

C. RUN PROCEDURE

With filling completed, the system was ready to be run. The standard run procedure was as follows:

a. Open cooling water supply valve and valve to bearing cooling water line.

b. Start the cooling water pump and adjust the pump output pressure regulator to set the rotameter reading at thirty percent.

c. Oil the evaporator bearing.

d. Energize and start the drive motor. Increase speed to 1100 RPM and insure the annulus has formed in the evaporator.

e. Set rotational speed to the desired value.

f. Let the system reach steady state and take zero power thermocouple readings and cooling water flow rate, also noting the tachometer reading.

g. Set power to heater to desired level and allow the system to come to steady state. Take tachometer, cooling water flow rate, and thermocouple readings.

h. Repeat step g. for each power level desired.

i. Repeat step f.

The only variation from this run procedure was when the transient response was taken. With the system running at a given rotational speed and an input power of two kilowatts, the power was instantaneously secured. Vapor thermocouple readings were recorded at specific intervals of time from

the step change in power. This process was also repeated for the case of instantaneously increasing power from zero to two kilowatts.

D. DATA REDUCTION

Data was reduced by first correcting the actual thermocouple readings using the calibration curves and then converting the voltage readings to degrees Fahrenheit using copper-constantan thermocouple conversion tables. Percent flow rate was converted to pounds per hour using the rotameter calibration curve. Heat transfer for each run was calculated as the product of the cooling water mass flow rate, the difference in temperature between cooling water inlet and outlet, and the specific heat of the cooling water, assumed to be one BTU per pound per degree Fahrenheit. To correct for heat generated by friction in the garlock seals and that due to viscous dissipation of the cooling water, the average zero power heat transfer rate was subtracted from the calculated heat transfer rate.

To find the predicted heat transfer rate, the voltage readings of the condenser wall thermocouples were corrected and converted to degrees Fahrenheit. These temperatures and their corresponding longitudinal position along the condenser were input to a least squares polynomial approximating computer program. The second order polynomial obtained from this program was used as an input to the theoretical program. Other inputs to the theoretical program were saturation

temperatures, rotational speed, properties of the working fluid and geometry and properties of the condenser. The theoretical program gave a predicted heat transfer rate as output.

Both experimental and theoretical heat transfer rates were plotted as functions of saturation temperature. Condenser temperature was plotted as a function of longitudinal position on the condenser and the approximating polynomials were plotted on the same graphs to show how the approximation compared to the actual data.

In the transient response runs, the saturation thermocouple voltage readings were corrected, converted to degrees Fahrenheit, and plotted as a function of time.

IV. PRESENTATION AND DISCUSSION OF RESULTS

A. REPEATABILITY OF RESULTS

A plot of heat transfer rate versus saturation temperature for several different runs is presented in Figure 5. Note that there is very good repeatability even though three different fill techniques were used and the system was allowed to set idle for twenty-four hours between filling and running in one case. The difference between these runs however, is greater than the experimental error so the physical characteristics did change with each fill.

B. EFFECTS OF NONCONDENSABLE GASES

The standard fill procedure was used for this study, but the interior pressure of the thermosyphon was deliberately kept at one micron of mercury at the time it was sealed leaving some noncondensable gases in the thermosyphon. The thermosyphon was run at 700 and 2800 RPM. The system was then vented to remove the noncondensable gases and the runs at 700 and 2800 RPM were repeated. Figure 6 shows a comparison of these runs.

The presence of noncondensable gases in the condenser reduces the heat transfer rate of the heat pipe. When running with noncondensables present, what appeared to be a dry area of condenser wall was observed through the viewports. This area extended from the endpiece for about one inch along the condenser wall all around the circumference

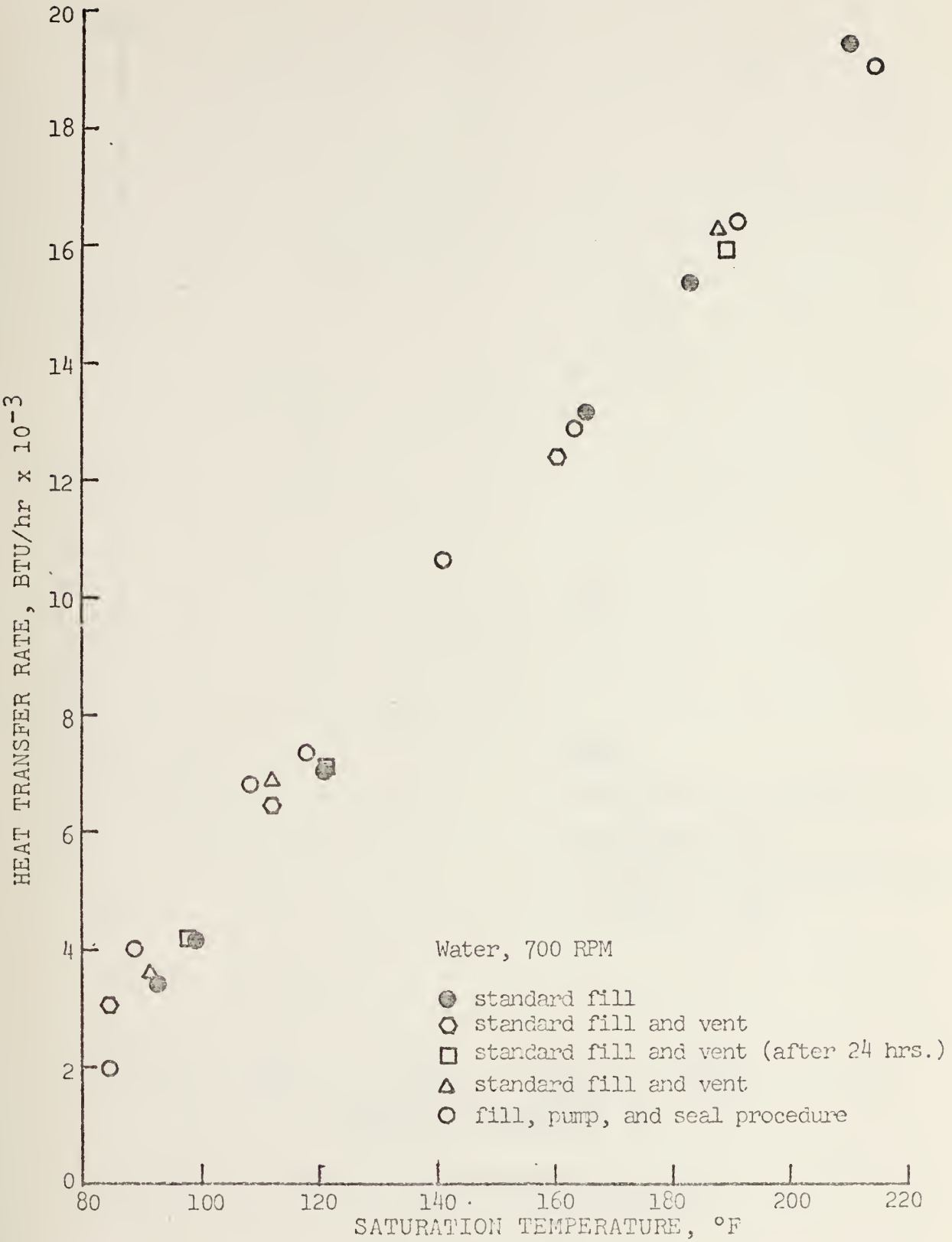

Figure 5. Comparison of Filling Procedures

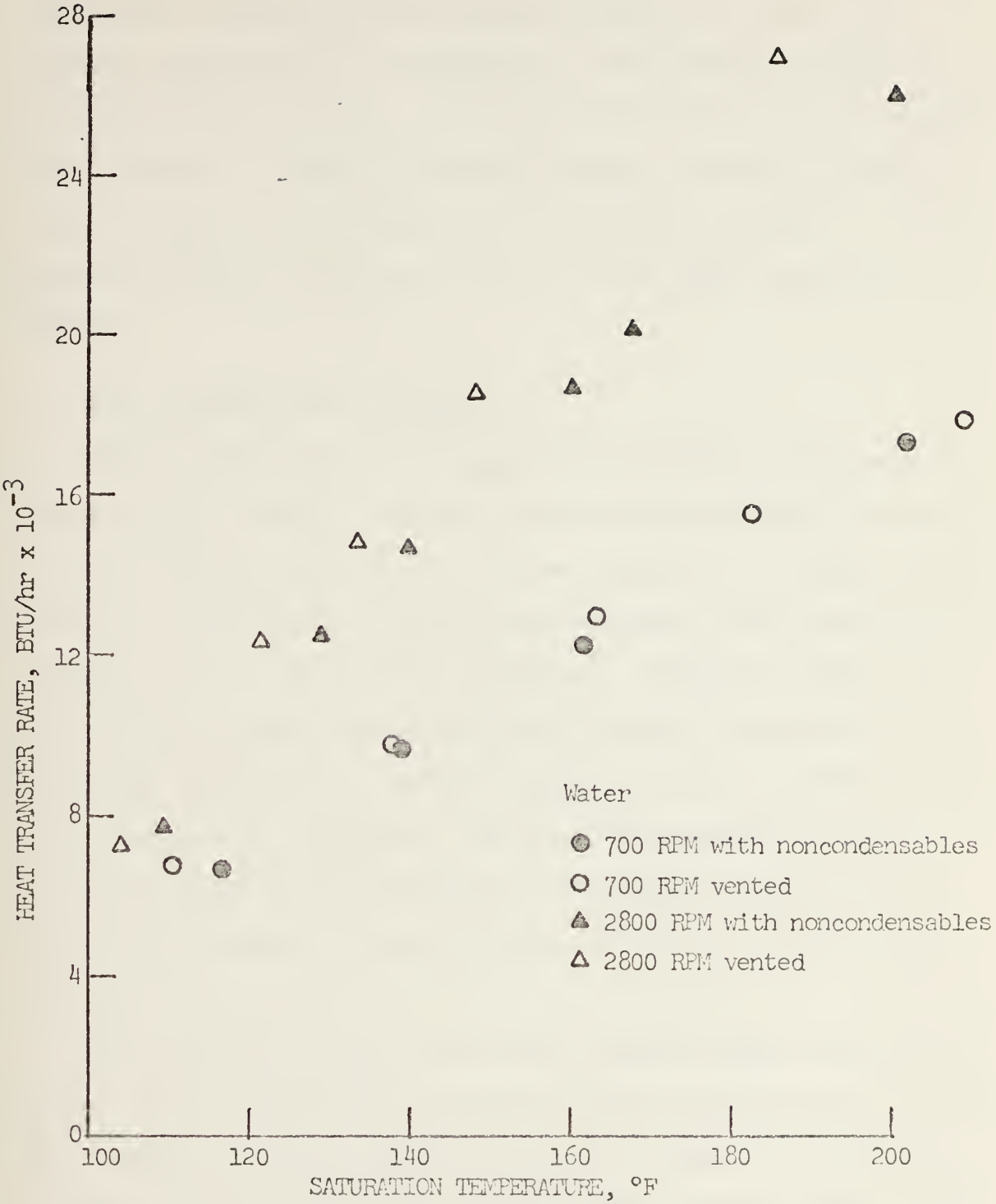

Figure 6. Effects of Noncondensable Gases:

of the condenser. This effect was probably the noncondensable gases blanketing the condenser wall, reducing the surface available for condensation, and thereby reducing the heat transfer rate. A greater reduction in heat transfer rate occurred at high rotational speeds, probably because the increased centrifugal force caused the blanket of noncondensables to flatten out over even more condenser surface.

C. WALL TEMPERATURE PROFILES

Three different wall temperature profiles are shown in Figures 7, 8, and 9. Distance zero corresponds to the end of the condenser farthest from the evaporator. Temperatures would be expected to continuously increase with increasing distance from the condenser endpiece. Figure 7, which is a profile for zero power input and 700 RPM, shows that the temperature reaches a minimum somewhere near the middle of the condenser. The reason for this discrepancy is due to the frictional heat generated by the Garlock seal located near the condenser endpiece which raised the temperature at this end.

The effects of this frictional heating were expected to become less significant as heater power was increased. This was exactly what did happen as shown in Figure 8 which is a profile at five kilowatts heater power and 700 RPM. Note that in this case the temperature is greater at the evaporator end than at the xero end of the condenser and that the low point of the temperature profile has moved toward the zero end.

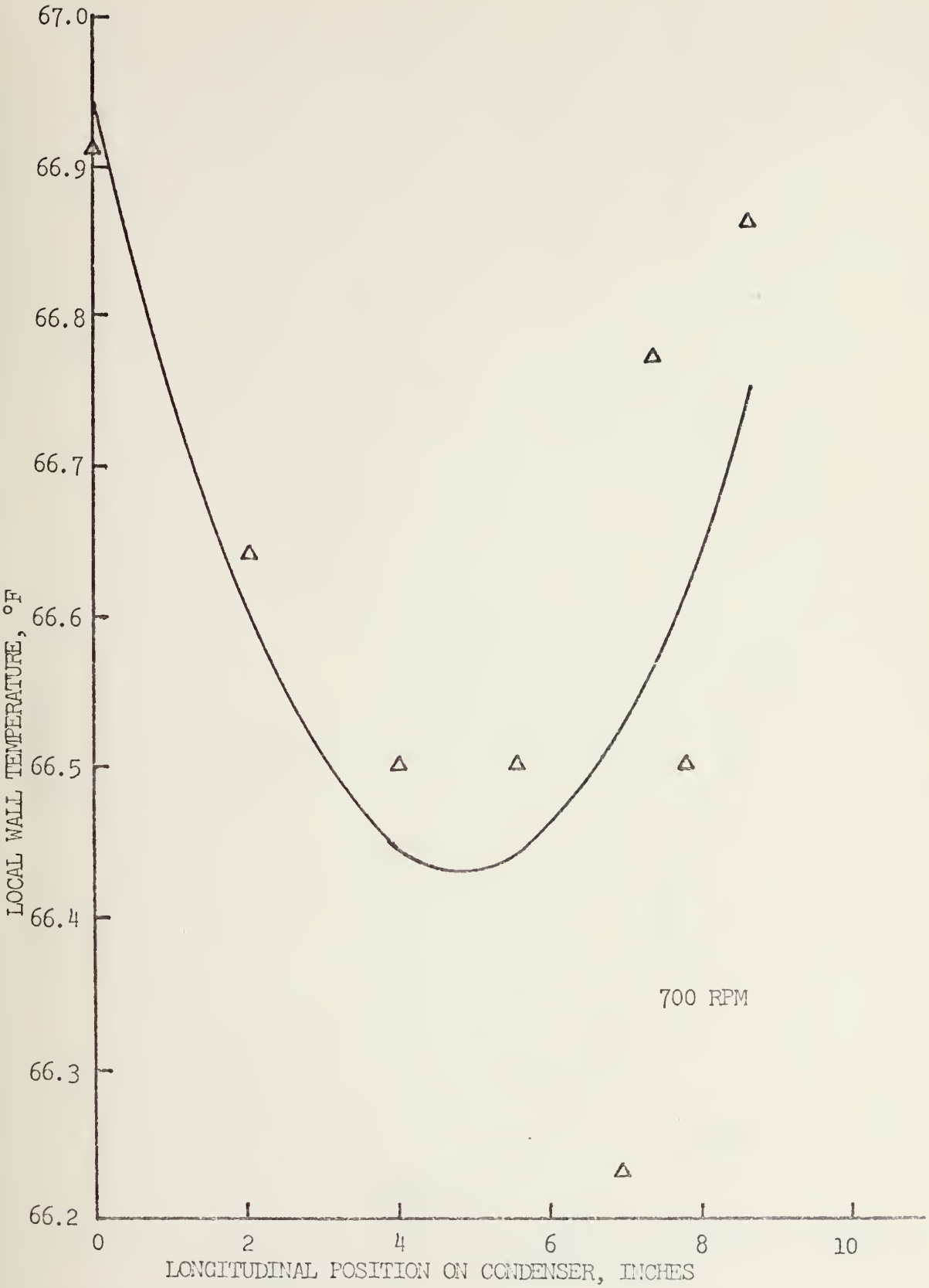

Figure 7. Wall Temperature Profile for Water at Zero Power and Low Speed

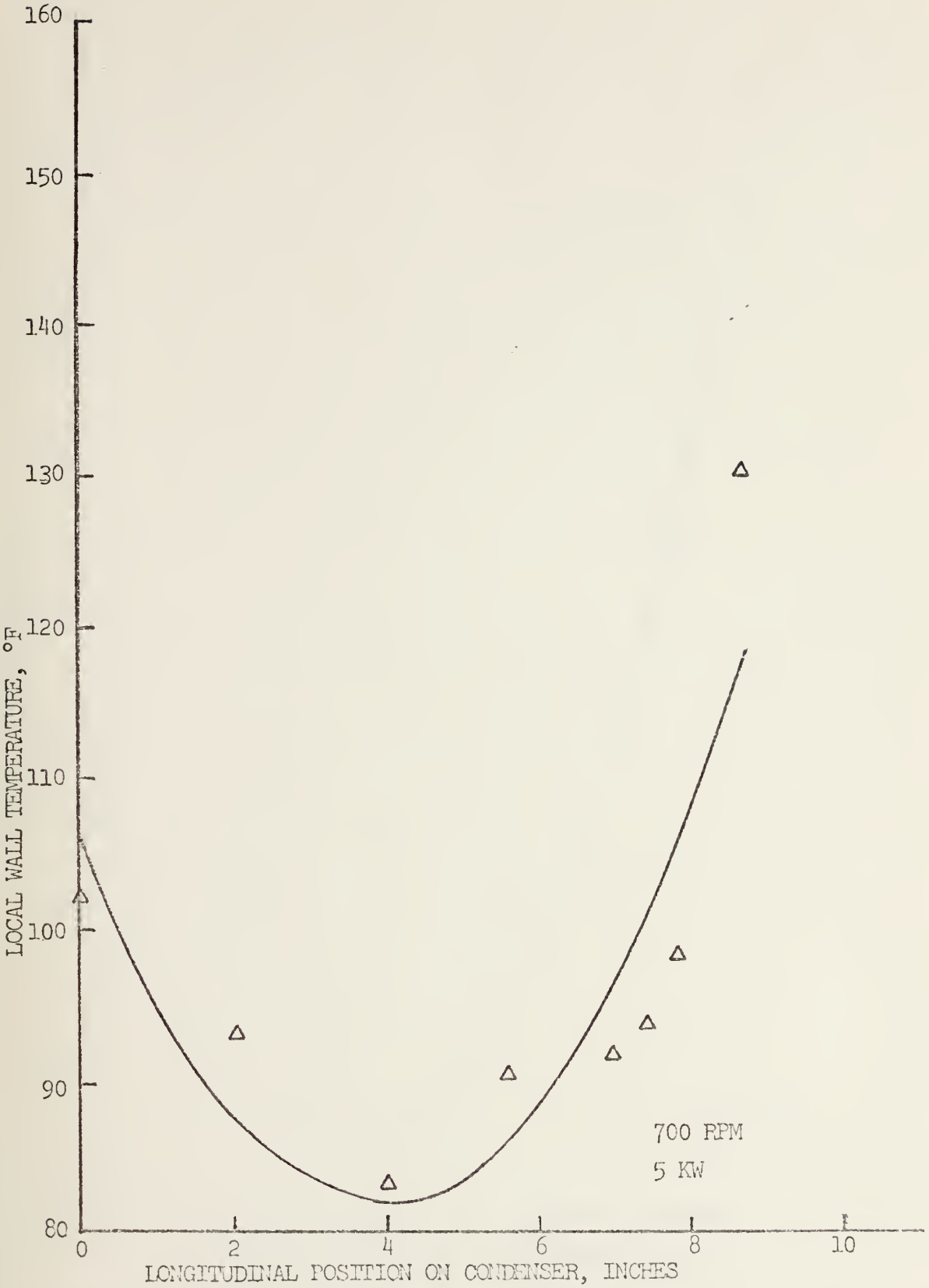

Figure 8. Wall Temperature Profile for Water at High Power and Low Speed

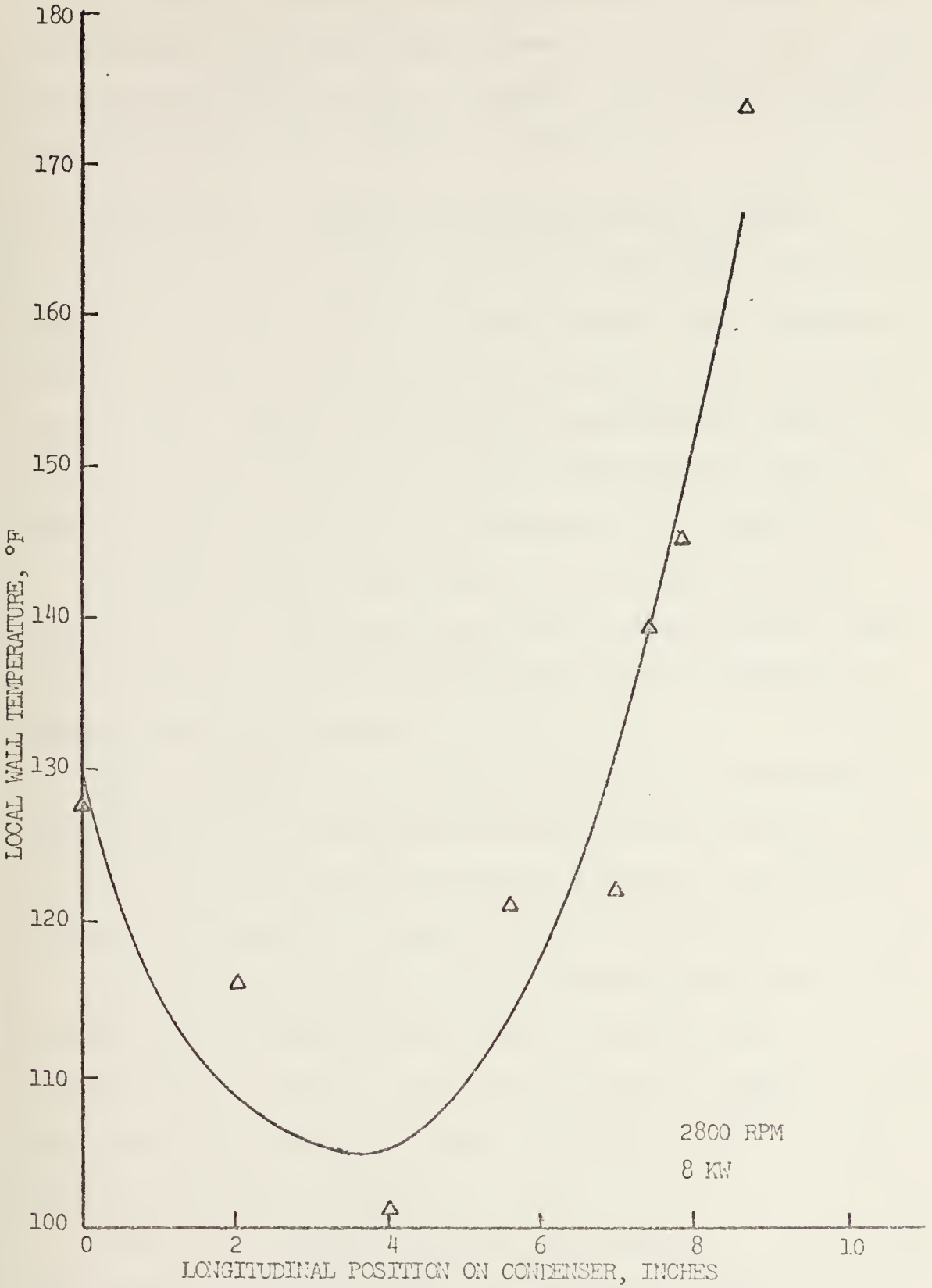

Figure 9. Wall Temperature Profile for Water at High Power and High Speed

At higher rotational speeds, even more frictional heat is generated, although higher power levels are also possible so that the profile shown in Figure 9 for eight kilowatts and 2800 RPM is very similar to Figure 8.

D. COMPARISON OF PREDICTED AND EXPERIMENTAL RESULTS

Runs were made at 700, 1400, and 2800 RPM, using water, ethanol, and freon 113 as working fluids. The equipment was filled by the standard fill procedure and vented for each of these runs. Graphs depicting the experimental results and the predicted results for 700 and 2800 RPM runs with all three fluids are presented in Figures 10, 11, and 12.

The experimental heat transfer rate was less than predicted when water was used as the working fluid. Also, the agreement between experiment and theory improved at higher rotational speeds.

Using ethanol as the working fluid, the experimental performance was significantly greater than predicted. Again in this case the agreement between experiment and theory appears to improve at greater rotational speeds.

In the case of freon 113, the theoretically predicted results and the experimental results agree within the experimental accuracy. The trend to better agreement between experiment and theory at higher rotational speed is less obvious but still appears to occur.

There are a number of possible reasons for the disagreement between the experiment and predicted results. One

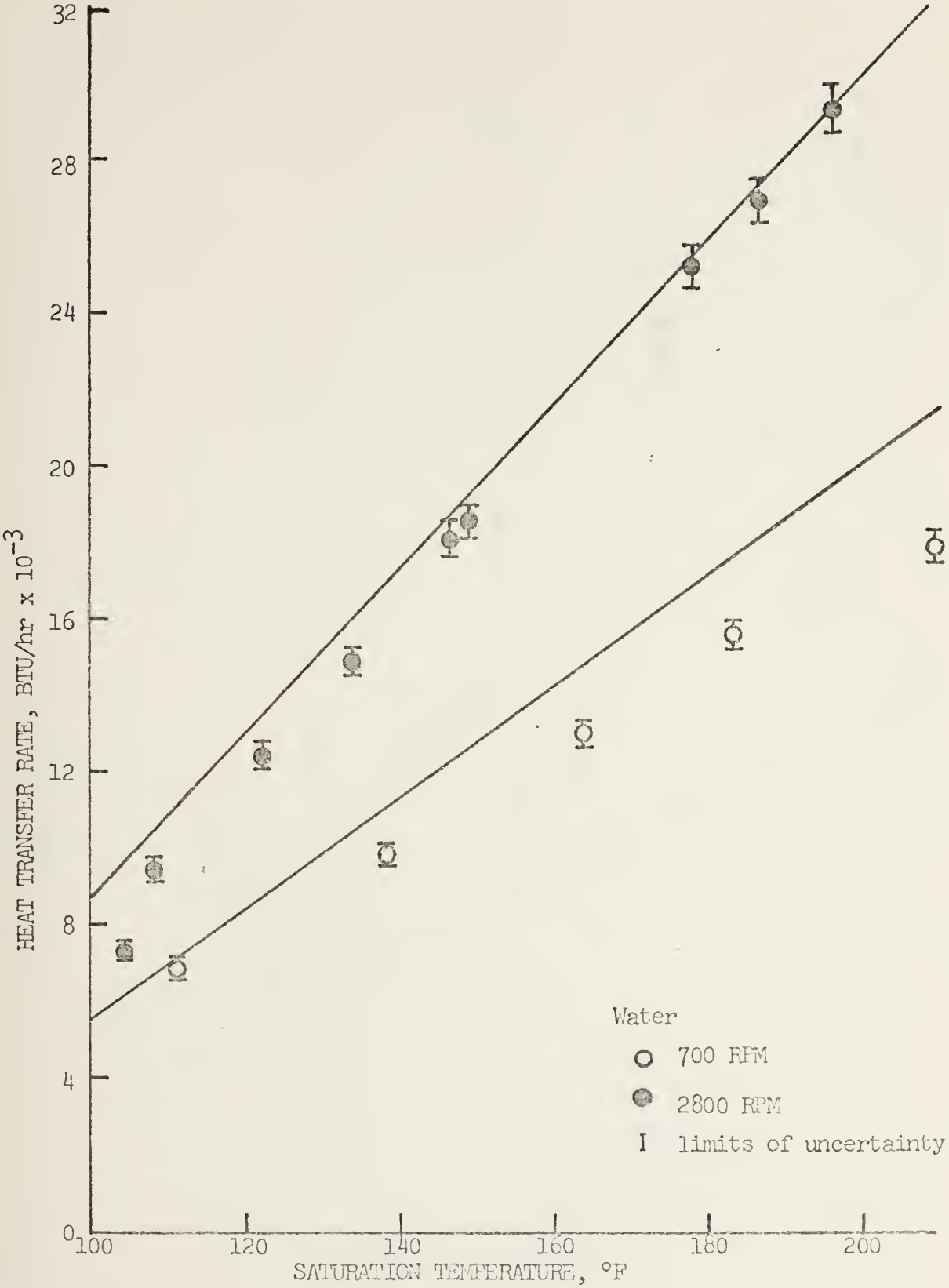

Figure 10. Heat Transfer Rate versus Saturation Temperature for Water

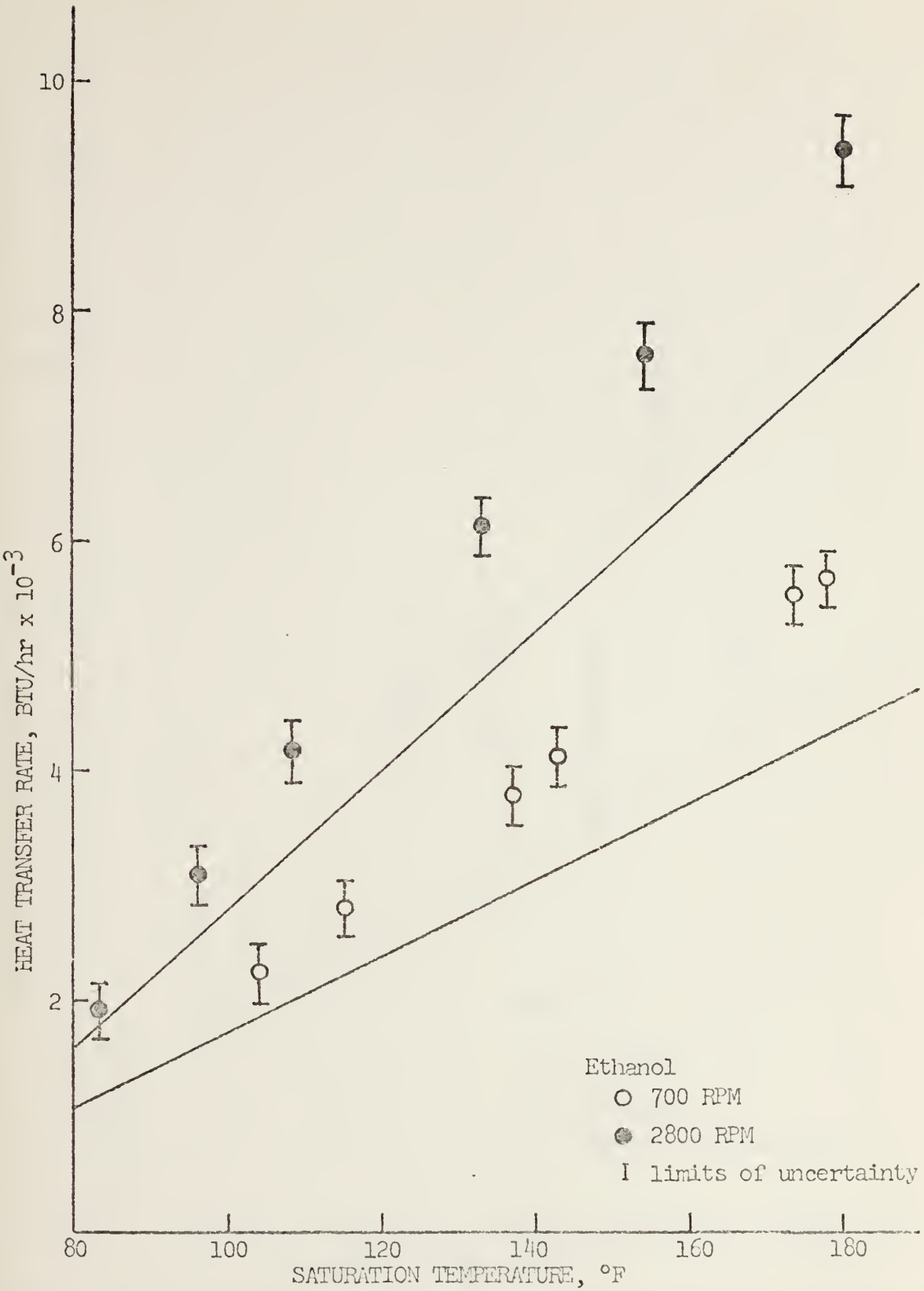

Figure 11. Heat Transfer Rate versus Saturation Temperature for Ethanol

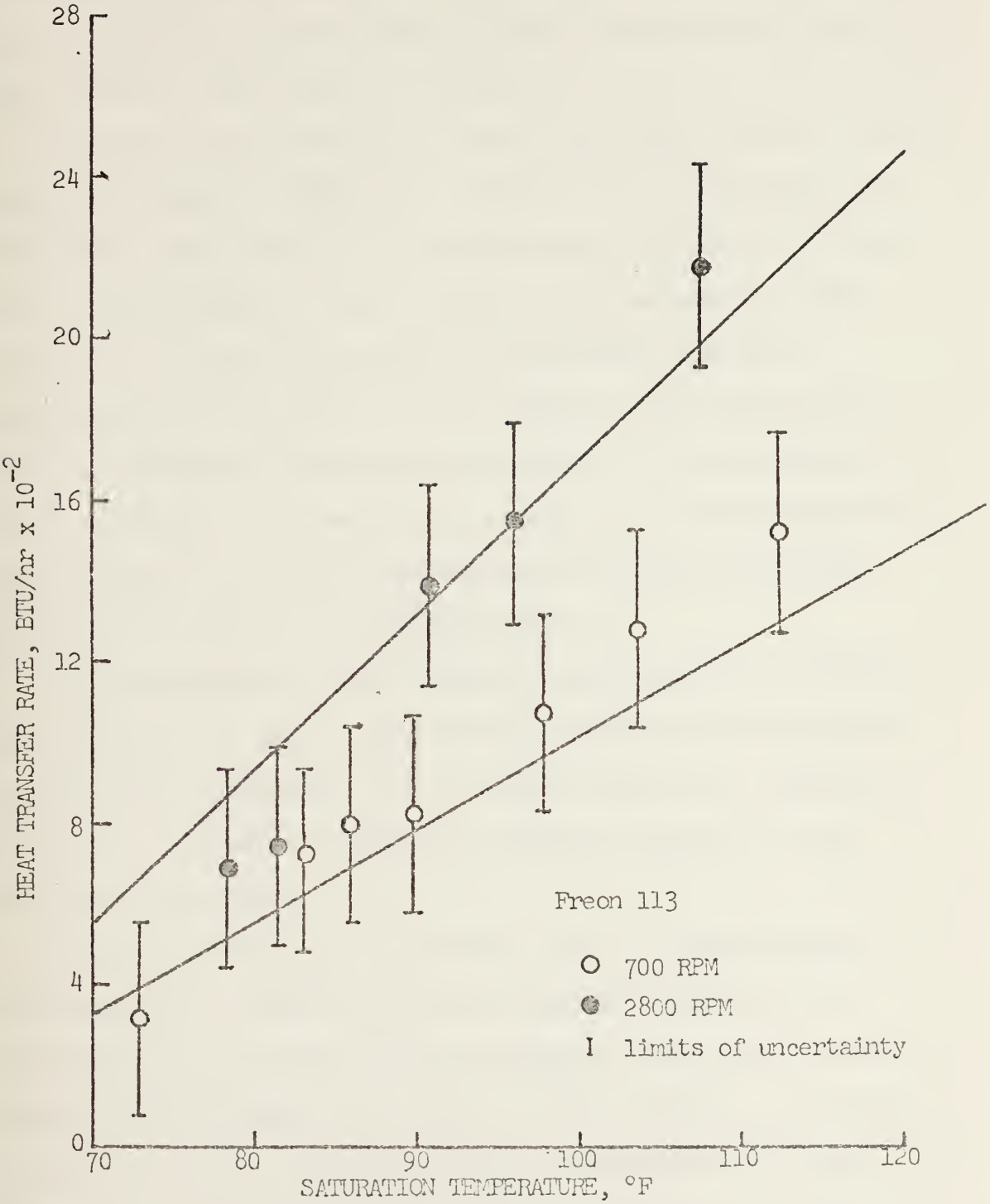

Figure 12. Heat Transfer Rate versus Saturation Temperature for Freon 113

reason why the experimental data is less than predicted might be that the vapor traveling up the center of the condenser is entraining the returning condensate, building up a thicker condensate layer thereby reducing the rate of heat transfer from the condenser.

Comparing the predicted vapor velocities for all three working fluids at saturation temperatures near 100°F and 2800 RPM, water vapor is traveling approximately 47 feet per second, ethanol vapor 6.8 feet per second and freon vapor at 1.3 feet per second. The higher velocity experienced using water as the working fluid would lead to more entrainment of condensate and hence to an experimental heat transfer rate lower than predicted. At the relatively lower vapor velocities experienced by ethanol and freon, entrainment might not be significant.

At greater rotational speeds, the greater centrifugal force on the returning condensate could be overcoming the entrainment phenomenon. This would lead to the improved agreement at higher rotational speeds observed in the results for water.

A second possible explanation for the experimental heat transfer rates being lower than predicted involves the condition at the exit of the condenser where the condensate returns to the evaporator over a sharp corner. In studying a similar corner situation, Nimmo and Leppert [7] found that a smooth, rounded corner and a fluid with low surface

tension result in a relatively thin film upstream of the corner. Increasing the surface tension of this fluid increases the upstream film thickness and replacing the rounded corner with a squared corner, such as the one used in this experiment, tends to exaggerate the surface tension effect.

At 100°F, the surface tensions for water, ethanol and freon 113 are .005, .0015, and .0015 pounds force per foot respectively. Therefore, the relatively high surface tension of water, exaggerated by the squared corner could mean the thickness of the water film in the condenser is greater than predicted, leading to heat transfer rates less than predicted. At the lower surface tension values of ethanol and freon 113 this effect of the corner shape on film thickness would be less significant.

The theoretical analysis is based on the assumption that the condensate film is laminar. Any turbulence in this film would increase the heat transfer rate. In addition Bird, Steward, and Lightfoot [8] found that even ripples on the surface of an otherwise laminar film increase the heat transfer rate. This could explain how the experimental heat transfer rates could exceed the predicted values. The increased centrifugal force on the condensate film at increased rotational speeds could be causing the film to behave in a more laminar manner, accounting for the slightly better agreement between experiment and theory at higher rotational speeds.

Another assumption made for the theoretical analysis is that all condensation takes place on the condenser wall, ignoring any condensation on the condenser endpiece, or glass viewport. The fact that some condensation did occur on these surface could further explain the cases where the experimental heat transfer rate was greater than predicted. Furthermore, at increased rotational speeds, with increased heat transfer rates, this heat transfer out the ends would be a less significant part of the total heat transfer, leading to the improvement in agreement at higher RPM.

One last possible source of disagreement between the experimental and predicted heat transfer rates is the assumption that the one inch section of the heat pipe between the evaporator and condenser was adiabatic and at the saturation temperature. If there was a significant amount of heat transfer through this section it would introduce some disagreement between the experiment and the theory.

E. COMPARISON OF WORKING FLUIDS

In addition to the results shown in Figures 10, 11, and 12, runs using each of the three working fluids were conducted at 1400 RPM. As shown in Figure 13, water gave the highest heat transfer rates, and freon 113 the lowest, for a given saturation temperature. The relatively high heat of vaporization and high thermal conductivity of water undoubtedly accounted for this superior performance.

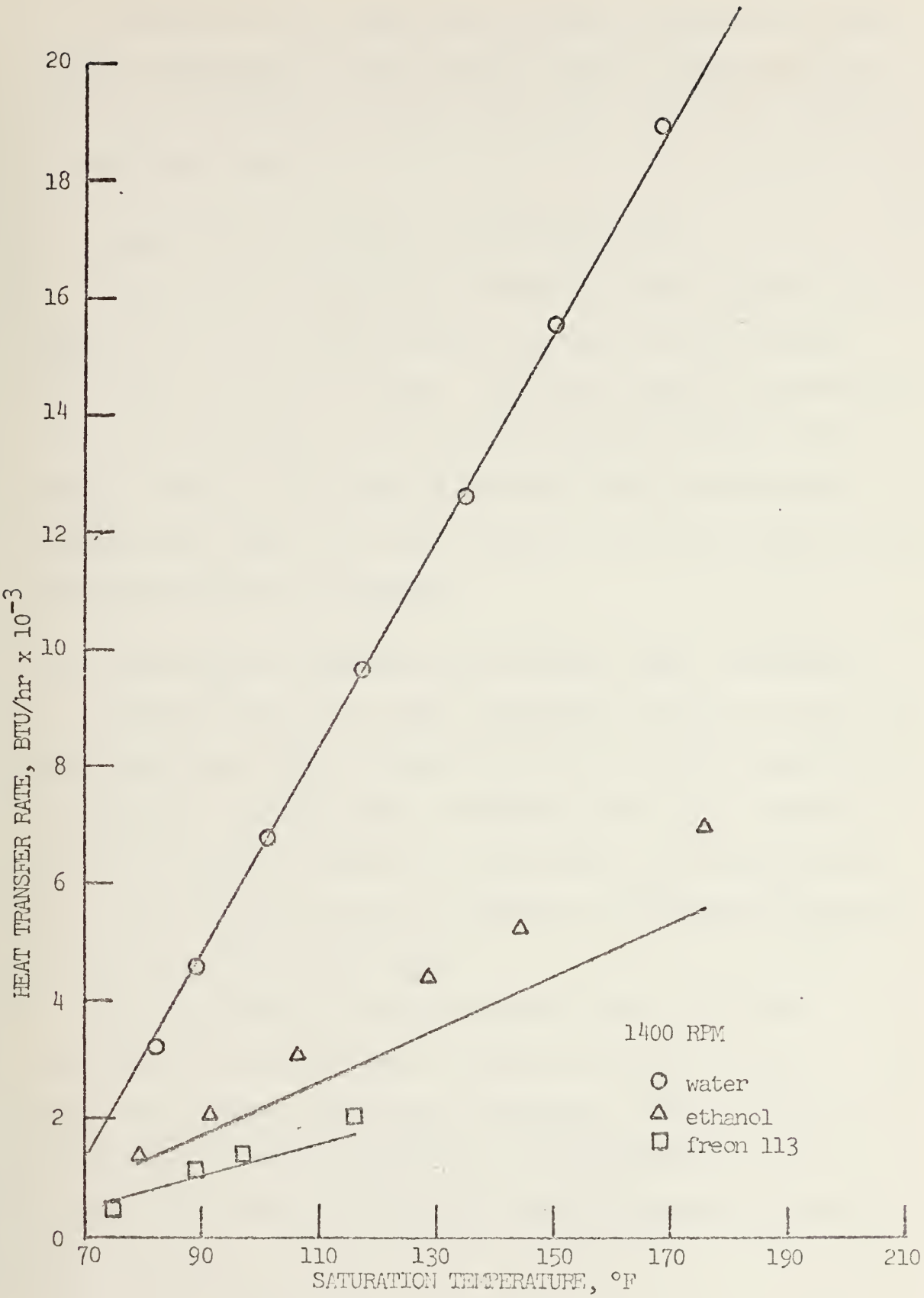

Figure 13. Comparison of Working Fluids

The runs at 1400 RPM seemed to give smoother data and better agreement with the theory, possibly because 1400 RPM is an operational speed where there is lower vibration in the heat pipe.

F. COMPARISON OF PRESENT AND PREVIOUS DATA

The results obtained by Schafer [4] are compared in Figure 14 to the present results using the same copper condenser filled with water. The most logical explanation for the difference in the results is that Schafer had a vacuum leak in his condenser section which allowed non-condensable gases into the condenser section, deteriorating the thermosyphon performance.

G. COMPARISON OF COPPER AND STAINLESS STEEL CONDENSERS

Installation of a copper condenser section in place of the stainless steel condenser used in previous experiments resulted in a significant increase in the heat transfer rate, as shown in Figure 15. This was as expected since the thermal conductivity of copper is considerably greater than that of stainless steel.

The difference in heat transfer rate of the two condensers became larger at higher rotational speeds. This was also expected since the condensate film is thinner at these higher speeds making the wall resistance a more significant part of the total thermal resistance across the condenser.

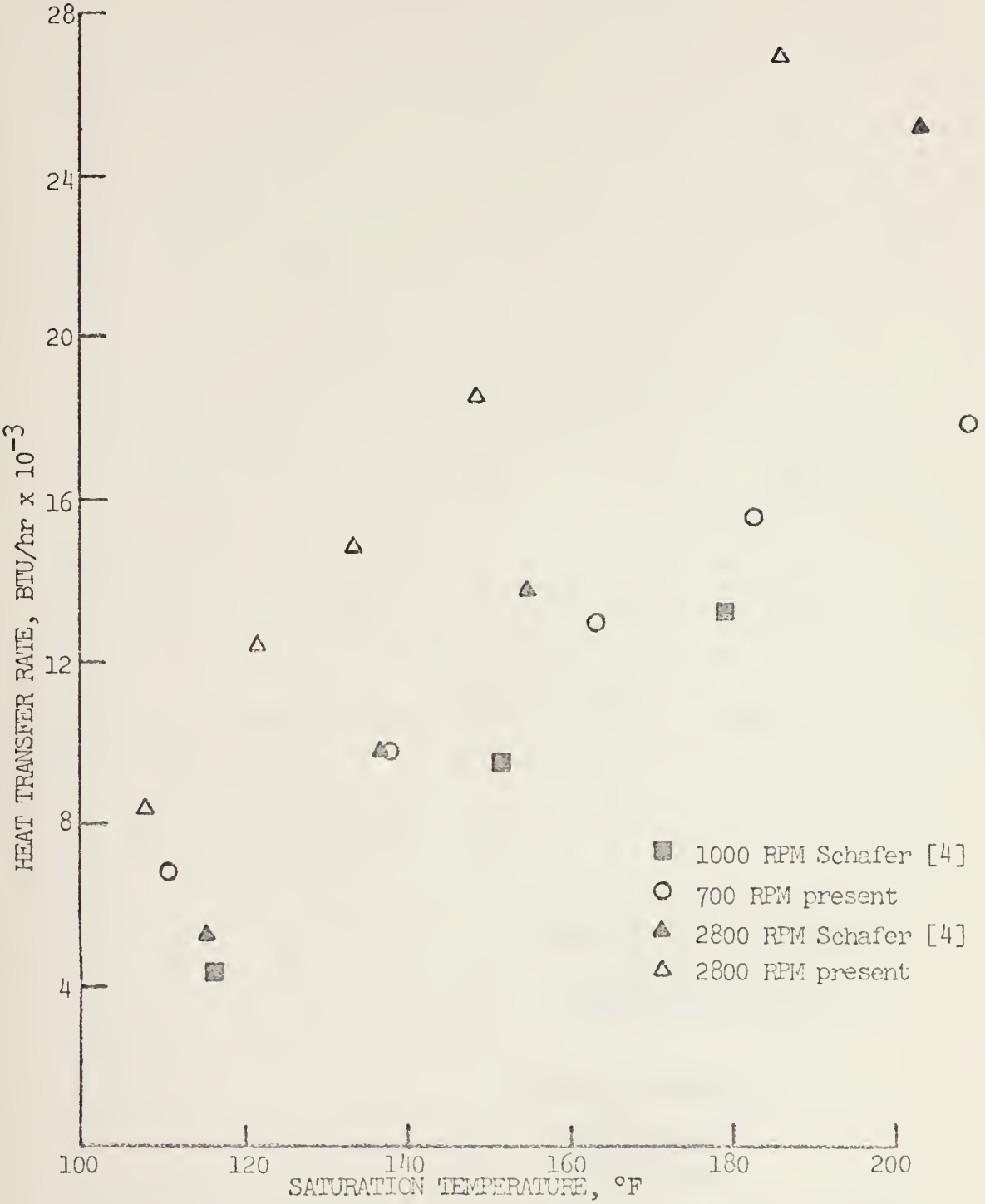

Figure 14. Comparison of Experimental Results with Experimental Results of Schafer [4]

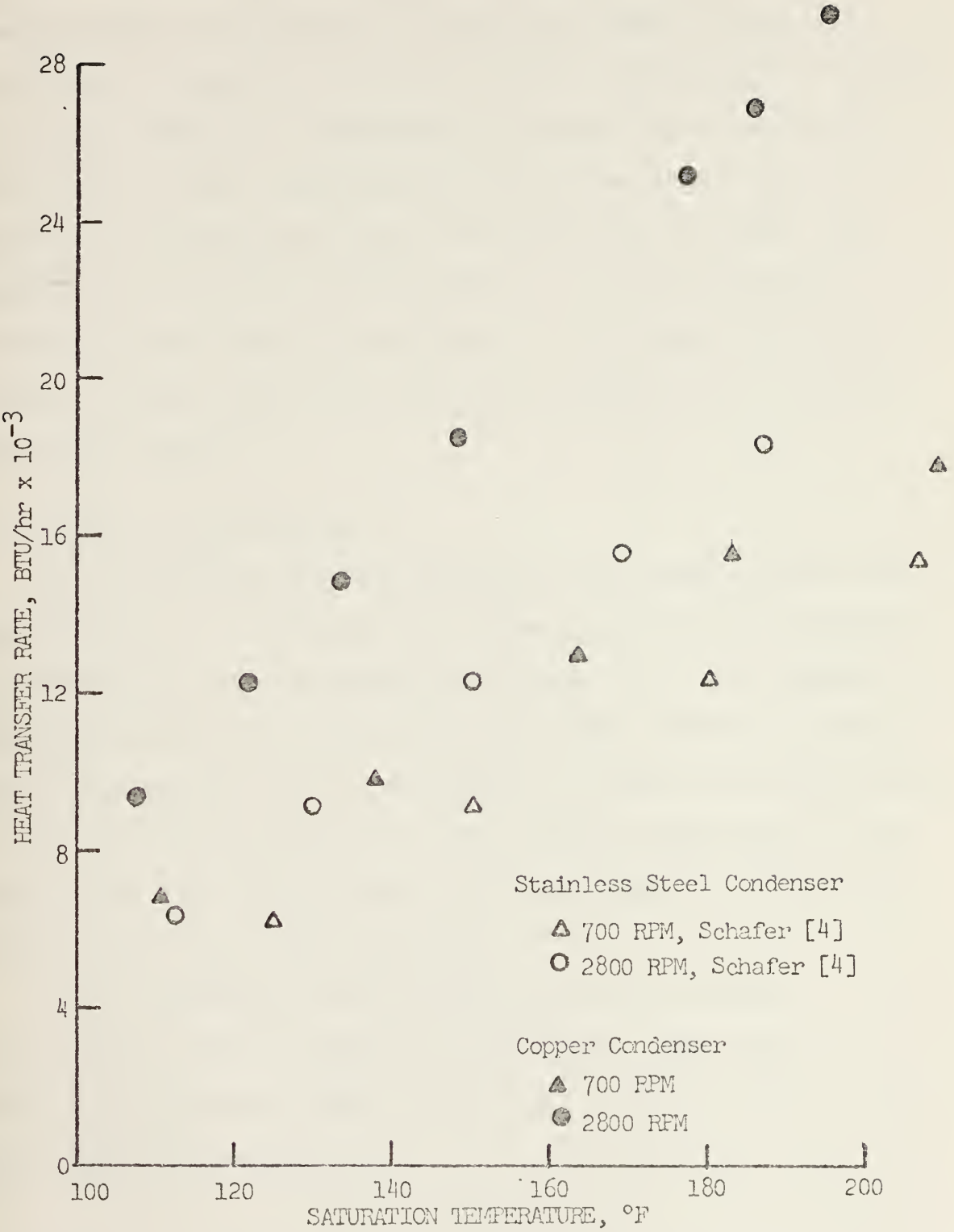

Figure 15. Comparison of Experimental Results for Copper and Stainless Steel Condensers

H. TRANSIENT RESPONSE

The transient response of the vapor temperature to a two kilowatt step change in evaporator power is presented in Figures 16 and 17. One would expect a more rapid response at higher rotational speeds due to better condensation but the plots of vapor temperature versus time show that the response at 2800 RPM is much slower than at 700 RPM. One possible explanation of this effect is that entrainment effects might be more predominant at the higher rotational speeds, slowing down the returning condensate and therefore the whole cycle.

I. DROPWISE CONDENSATION

Two separate runs were devoted to the study of dropwise condensation. A comparison of these two runs and a filmwise condensation run is presented in Figure 18. The increase in heat transfer rate achieved by going from filmwise to dropwise condensation was as anticipated. While the repeatability of the dropwise condensation data was not expected to be as good as in the filmwise case, the large differences between the dropwise runs were surprising.

These differences were almost surely the result of inconsistent application of the promoter. The nature of the silicone grease made it difficult to apply evenly with any degree of consistency.

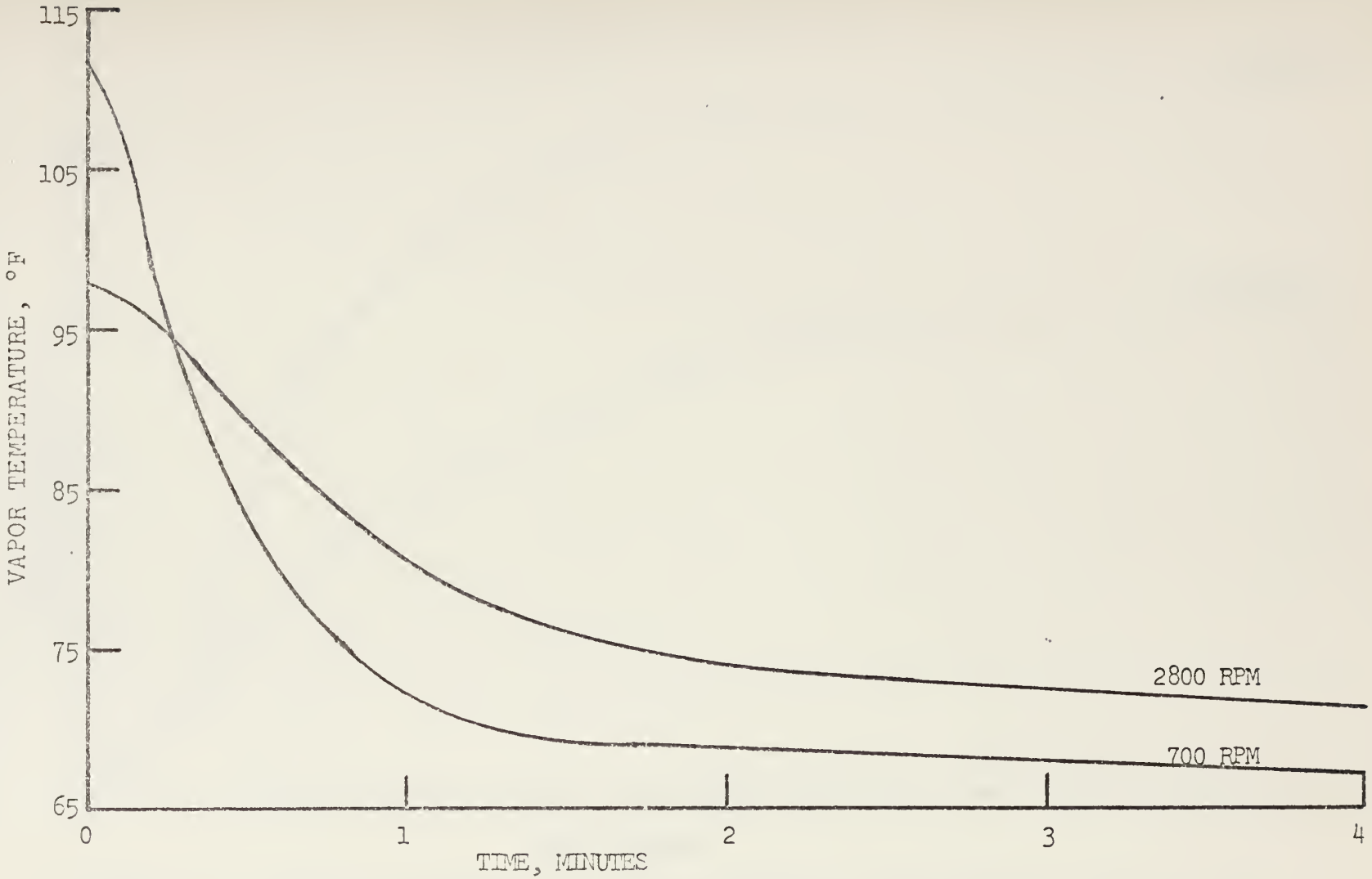

Figure 16. Transient Response to a Step Change in Power from 2 KW to 0 KW

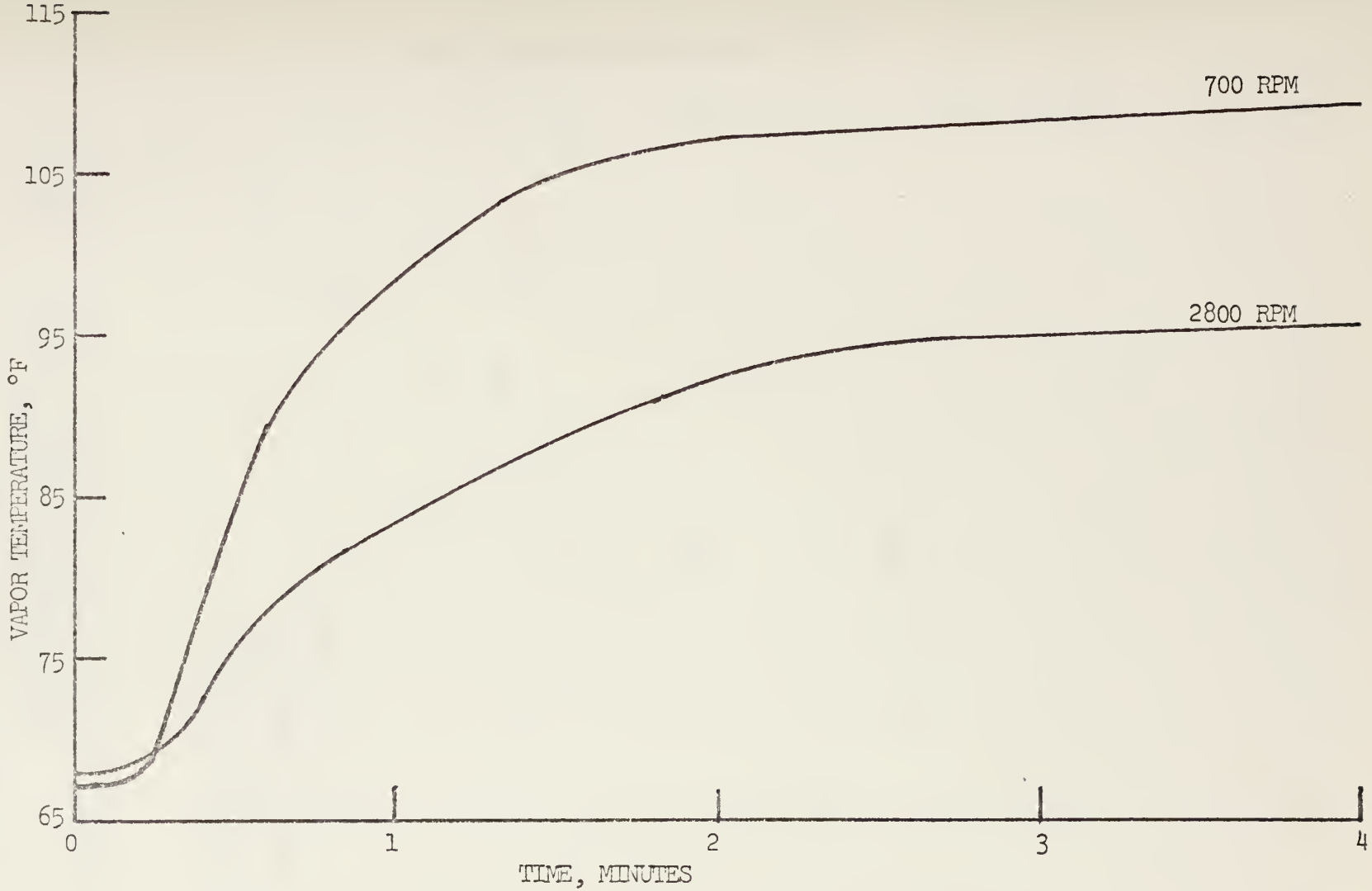

Figure 17. Transient Response to a Step Change in Power from 0 KW to 2 KW

Figure 18. Comparison of Experimental Results for Filmwise Condensation and Dropwise Condensation

V. CONCLUSIONS AND RECOMMENDATIONS

A. CONCLUSIONS

There are several conclusions to be drawn from the experimental results. First the presence of noncondensable gases in the thermosyphon reduces the heat transfer rate, depending upon the volume of noncondensable gas present. Also, the effects of these noncondensables are more pronounced at higher rotational speed.

There is reasonable agreement between theory and experiment for working fluids water, ethanol and freon 113. This agreement improves as the rotational speed increases.

The highest heat transfer rates are achieved using water as the working fluid and freon 113 gives the lowest heat transfer rates. The heat transfer rate is higher for the copper condenser than for the stainless steel condenser.

Promoting dropwise condensation greatly increases the heat transfer rate of the thermosyphon. However, a more reliable means of promoting dropwise condensation is needed before a valid comparison of dropwise and filmwise condensation can be made.

B. RECOMMENDATIONS

There are several interesting areas for further work on the thermosyphon. Some of them are:

a. Further study of noncondensable gas effects from both a theoretical and experimental approach.

b. Further investigation of the condenser corner effect and incorporation of surface tension effects into the theoretical model. Also the shape of the corner could be changed and its effect on the experimental results noted.

c. Further investigation of dropwise condensation with special emphasis on finding a good promoter and achieving repeatable results.

d. Further study of transient response for all three working fluids under various conditions.

APPENDIX A

UNCERTAINTY ANALYSIS

The method of Kline and McClintock [9] was used to estimate the uncertainties in the experimental heat transfer rates. The basic equations used were:

$$q_T = \dot{m}\, c_p\, \Delta T$$
$$q_{hl} = \dot{m}\, c_p\, \Delta T_{hl}$$
$$q_c = q_T - q_{hl}$$

where:

q_T = total uncorrected heat transfer rate

q_{hl} = heat transfer rate due to extraneous sources of heat such as bearing friction, etc.

q_c = corrected heat transfer rate

$\dot{m}$ = mass rate of flow of the cooling water

c_p = specific heat of the cooling water

ΔT = the change in temperature of the cooling water

ΔT_{hl} = the change in the temperature of the cooling water caused by extraneous heat sources

Using subscripted w's to indicate the uncertainties, the fractional uncertainty in the uncorrected heat transfer rate is given by:

$$\frac{w_{q_T}}{q_T} = \sqrt{\left(\frac{w_{\dot{m}}}{\dot{m}}\right)^2 + \left(\frac{w_{c_p}}{c_p}\right)^2 + \left(\frac{w_{\Delta T}}{\Delta T}\right)^2}$$

The fractional uncertainty in the extraneous heat transfer rate is calculated by the same kind of equation:

$$\frac{w_{q_{hl}}}{q_{hl}} = \sqrt{\left(\frac{w_{\dot{m}}}{\dot{m}}\right)^2 + \left(\frac{w_{c_p}}{c_p}\right)^2 + \left(\frac{w_{\Delta T_{hl}}}{\Delta T_{hl}}\right)^2}$$

The uncertainty in the corrected heat transfer rate is given by:

$$w_{q_c} = \sqrt{w_{q_T}^2 + w_{q_{hl}}^2}$$

The specific heat of the cooling water and its associated uncertainty were considered constant throughout the tests.

$$c_p = 1.000 \text{ BTU/lbm } ^\circ\text{F}$$

$$w_{c_p} = \pm 0.002 \text{ BTU/lbm } ^\circ\text{F}$$

The mass flow rate of the cooling water was set to the same value for each run, therefore the uncertainty in this mass flow rate was always the same.

$$\dot{m} = 1094 \text{ lbm/hr}$$

$$w_{\dot{m}} = \pm 20 \text{ lbm/hr}$$

ΔT and ΔT_{hl} varied considerably but since these values both depended on readings taken from the cooling water inlet

and outlet thermocouples, the uncertainties for both values were the same.

$$w_{\Delta T} = \pm 0.2\ ^\circ F$$

$$w_{\Delta T_{hl}} = \pm 0.2\ ^\circ F$$

The following is a sample error analysis calculation at 700 RPM and 3.984 KW input power where:

$$q_T = 13{,}784\ \text{BTU/hr}$$

$$\dot{m} = 1094\ \text{lbm/hr}$$

$$c_p = 1.0\ \text{BTU/lbm}\ ^\circ F$$

$$\Delta T = 12.60\ ^\circ F$$

$$\frac{w_{q_T}}{q_T} = \sqrt{\left(\frac{w_{\dot{m}}}{\dot{m}}\right)^2 + \left(\frac{w_{c_p}}{c_p}\right)^2 + \left(\frac{w_{\Delta T}}{\Delta T}\right)^2}$$

$$\frac{w_{q_T}}{13{,}784} = \sqrt{\left(\frac{20}{1094}\right)^2 + \left(\frac{.002}{1.0}\right)^2 + \left(\frac{0.2}{12.60}\right)^2}$$

$$w_{q_T} = 13{,}784 \sqrt{.0005901}$$

$$w_{q_T} = \pm 334.8\ \text{BTU/hr}$$

For this run, it was determined that the heat transfer due to extraneous sources was:

$$\Delta T_{hl} = 0.75^\circ F$$

$$q_{hl} = 815.0\ \text{BTU/hr}$$

therefore

$$\frac{w_{q_{hl}}}{q_{hl}} = \sqrt{\left(\frac{w_{\dot{m}}}{\dot{m}}\right)^2 + \left(\frac{w_{c_p}}{c_p}\right)^2 + \left(\frac{w_{\Delta T_{hl}}}{\Delta T_{hl}}\right)^2}$$

$$w_{q_{hl}} = \sqrt{\left(\frac{20}{1094}\right)^2 + \left(\frac{.002}{1.0}\right)^2 + \left(\frac{0.2}{.75}\right)^2}$$

$$w_{q_{hl}} = 815.0 \sqrt{.072407}$$

$$w_{q_{hl}} = \pm 219.3 \text{ BTU/hr}$$

Then:

$$w_{q_c} = \sqrt{w_{q_T}^2 + w_{q_{hl}}^2}$$

$$w_{q_c} = \sqrt{(334.8)^2 + (219.3)^2}$$

$$w_{q_c} = \sqrt{160183.53}$$

$$w_{q_c} = \pm 400.2 \text{ BTU/hr}$$

Therefore the heat transfer rate at this data point is 12,969 BTU/hr ± 400 BTU/hr.

BIBLIOGRAPHY

1. Ballback, L.J., The Operation of a Rotating Wickless Heat Pipe, M.S. Thesis, Naval Postgraduate School, Monterey, California, December 1969.

2. Daley, T.J., The Experimental Design and Operation of a Wickless Heat Pipe, M.S. Thesis, Naval Postgraduate School, Monterey, California, June 1970.

3. Newton, W.H., Jr., Performance Characteristics of Rotating, Non-Capillary Heat Pipes, M.S. Thesis, Naval Postgraduate School, Monterey, California, June 1961.

4. Schafer, C.D., II, Augmenting the Heat Transfer Performance of Rotating Two-Phase Thermosyphons, M.S. Thesis, Naval Postgraduate School, Monterey, California, December 1972.

5. Woodard, J.S., The Operation of Rotating Non-Capillary Heat Pipes, M.S. Thesis, Naval Postgraduate School, Monterey, California, March 1972.

6. Smithells, C.J., Metals Reference Book, 3rd Ed., Vol. 2, p. 1030, Buttersworth, 1962.

7. Nimmo, B.G. and Leppert, G., Laminar Film Condensation on Finite Horizontal Surface, Clarkson College of Technology, Potsdam, New York, 1970.

8. Bird, R.B., Stewart, W.E., and Lightfoot, E.N., Transport Phenomena, John Wiley and Sons, Copyright 1960.

9. Kline, S.J., and McClintock, F.A., Describing Uncertainties in Single-Sample Experiments, Mechanical Engineering, January, 1953.

INITIAL DISTRIBUTION LIST

		No. Copies
1.	Defense Documentation Center Cameron Station Alexandria, Virginia 22314	2
2.	Library, Code 0212 Naval Postgraduate School Monterey, California 93940	2
3.	Department Chairman, Code 59 Department of Mechanical Engineering Naval Postgraduate School Monterey, California 93940	1
4.	Professor Paul J. Marto, 59Mx Department of Mechanical Engineering Naval Postgraduate School Monterey, California 93940	1
5.	LT. Richard S. Tucker, USN FLEACTS Detachment Box 1049 FPO Seattle 98761	1

153890
Thesis
T845 Tucker
c.1
Heat transfer characteristics of a rotating two-phase thermosyphon.